Atmos. Chem. Phys. Discuss., 9, 16483–16525, 2009
www.atmos-chem-phys-discuss.net/9/16483/2009/

Atmospheric Chemistry and Physics Discussions

This discussion paper is/has been under review for the journal *Atmospheric Chemistry and Physics (ACP)*. Please refer to the corresponding final paper in *ACP* if available.

The role of mixing layer on changes of particle properties in lower troposphere

L. Ferrero[1], E. Bolzacchini[1], M. G. Perrone[1], S. Petraccone[1], G. Sangiorgi[1], B. S. Ferrini[1], C. Lo Porto[1], Z. Lazzati[1], D. Cocchi[2], F. Bruno[2], and F. Greco[2]

[1]POLARIS research center, Department of Environmental Sciences, University of Milano-Bicocca, Piazza della Scienza 1, 20126, Milano, Italy
[2]Department of Statistics "P. Fortunati", University of Bologna, Via delle Belle Arti 41, 40126, Bologna, Italy

Received: 30 March 2009 – Accepted: 3 July 2009 – Published: 5 August 2009

Correspondence to: L. Ferrero (luca.ferrero@unimib.it)

Published by Copernicus Publications on behalf of the European Geosciences Union.

Abstract

Vertical profiles of atmospheric particulate matter number concentration, size distribution and chemical composition were directly measured in the city of Milan, over three years (2005–2008) of field campaigns. An optical particle counter, a portable meteorological station and a miniaturized cascade impactor were deployed on a tethered balloon. Mixing layer height was estimated by PM dispersion along height. More than 300 PM vertical profiles were measured both in the winter and summer, mainly in clear and dry sky conditions. Under these conditions, no significant changes in NO_3^-, SO_4^{2-} or NH_4^+ into or over the mixing layer were found. From experimental measurements we observed changes in size distribution along height. An increase of the mean particle diameter, in the accumulation mode, passing through the mixing layer under stable conditions was highlighted; the mean relative growth was 2.1±0.1% in the winter and 3.9±0.3% in the summer. At the same time, sedimentation processes occurred across the ML height for coarse particles leading to a mean particle diameter reduction (14.9±0.6% in the winter and 10.7±1.0% in summer). A hierarchical statistical model for the PM size distribution has been developed to describe the aging process of the finest PM fraction along height. The proposed model is able to estimate the typical vertical profile that characterises launches within pre-specified groups. The mean growth estimated on the basis of the model was 1.9±0.5% in the winter and 6.1±1.2% in the summer, in accordance with experimental evidence.

1 Introduction

Atmospheric particulate matter is crucial in environmental pollution problems, health hazards and climate changes. On one hand particulate matter is one of the most important atmospheric pollutants, specially in urban areas (Van Dingenen et al., 2004). Meteorological conditions, and in particular atmospheric turbulence play a relevant role in this way (Fischer et al., 2006); mixing layer height influences the PM exposure pat-

ACPD

9, 16483–16525, 2009

tern providing the available volume for the dispersion of aerosols and gases (Seibert et al., 2000). A typical example is the Po Valley (Northern Italy) where wind is scarce and stagnant conditions often occur causing a marked seasonally influenced PM trend (Rodriguez et al., 2007; Ferrero et al., 2007a; Vecchi et al., 2004).

On the other hand, it has been found that aerosols also influence the climatic system due to their ability to scatter and absorb sunlight (direct effect); particles in the atmosphere also act as cloud condensation nuclei (CCN) modifying the lifetime of clouds (Koren et al., 2004), droplet size and precipitation rate (indirect effect) (Kaufman et al., 2002). Globally they are opposed to greenhouse gases in global warming, cooling the earth-atmosphere system (IPCC, 2007). The number size distribution and the chemical composition of the particles in the atmosphere influence the optical properties of particulate matter and their ability to act as CCN (Kaufman et al., 2002; Penner et al., 2001; Hinds, 1999; Seinfeld, 1998).

The linkage between the particles' chemical-physical and their optical properties suggests the use of new tools, like satellite images in PM air pollution studies in order to spatialize the PM exposure pattern (Shaap et al., 2009; Engel-Cox et al., 2006; Liu et al., 2005, 2007; Sarigiannis et al., 2004) on anthropized areas in which a continuous monitoring activity of PM is not active, but where people live. Despite this possibility, aerosols in the atmosphere can vary greatly in their concentration, size and composition, and consequently in their effects on incident radiation (Campanelli et al., 2003).

So, climatic studies and the estimation of ground PM concentrations from satellites, require a 3-D knowledge of aerosol properties, especially along the whole atmospheric column (Wang et al., 2003; Kaufman et al., 1983). Measurements of particulate matter vertical distribution might therefore be very interesting, allowing us to understand the atmospheric processes related both with ground pollution levels (Seibert et al., 2000) and with vertical changes in aerosol optical properties. For this reason, due to the spatial heterogeneity of aerosol and atmospheric conditions, different behaviours of aerosol vertical properties have been described in the literature. For example, Campanelli

ACPD
9, 16483–16525, 2009

et al. (2003) reported that boundary layer thickness had no influence on changes in aerosol volume size distribution along height, while Hayasaka et al. (1998) demonstrated a connection between the columnar aerosol volume size distribution and details of the vertical profiles. These results explain well the effect of different aerosol vertical profiles employed in models on the indeterminacy in forecasting the aerosol radiative impact (Penner et al., 2001).

Up to now, direct long-term particle vertical property measurements are scarce (Penner et al., 2001) and those that exist, are limited to few points (Gobbi et al., 2004). As far as we know, this kind of measurement has not yet been the object of statistical modelling.

Vertical profiles of particulate matter can be obtained by direct and indirect techniques such as tethered balloons (McKendry et al., 2004; Stratmann et al., 2003; Maletto et al., 2003), aircrafts (that permit direct sampling) (Taubman et al., 2006), and lidars (indirect estimation) (Kim et al., 2007; Amiridis at al., 2007; Eresmaa et al., 2006). Among these, only direct techniques, like balloons, enable one to measure the physical-chemical properties of PM (number concentration, size distribution, chemical composition) and the effect of atmospheric turbulence on aerosol properties within the planetary boundary layer and across it (Seibert et al., 2000).

Following these routes, particulate matter vertical profiles were measured in Milan, within the Italian QUITSAT project (Air Quality in the Po Valley by Integrated measurements from Earth, Satellites and chemical and transport modelling), collecting three years of data. The main goal of the study consists in associating changes in the particle number concentration, size distribution and chemical composition along height with the mixing layer evolution. This was achieved by assessing the behaviour of particulate matter size distribution along vertical profiles by means of a statistical model. The hypotheses of such models are developed as a tool for eliciting the most relevant physical and chemical conjectures.

ACPD
9, 16483–16525, 2009

2 Site, instrumentation and statistical approach

Vertical profiles of atmospheric particulate matter were carried out at the urban site of Torre Sarca in Milan (45°31′19″ N, 9°12′46″ E – University of Milano-Bicocca). The site is located on the north side of Milan, in the middle of an extensive conurbation which is the most industrialized and populated one in the Po Valley.

2.1 Atmospheric particulate matter characterization

Vertical profiles of atmospheric particulate matter were carried out using a helium filled tethered balloon (Ø=4 m, 33.5 m^3) equipped with an optical particle counter (OPC), a miniaturized cascade impactor and a portable meteorological station deployed on a platform located 5 m away from the balloon (Fig. 1). An electric winch allowed us to control the ascent and descent rate of the balloon with a precision of 0.1 m/min; a fixed value of 30.0±0.1 m/min was used, giving a high spatial resolution of particle measurements (3.0 m of resolution for each 6 s OPC measurement) with a reasonable time of flight (10 min to reach 300 m a.g.l.). The maximum height reached by each balloon launch depended on the atmospheric conditions; for most profiles it ranged from 300 to 600 m a.g.l.

We used the OPC GRIMM *1.108 "Dustcheck"* that allowed us to measure the particle number size distribution in 15 classes from 0.3 μm to up to 20 μm. The instrument was also set to perform one measure every 6 s in order to reach a higher space resolution during the balloon flight. This OPC is also suitable for measuring vertical profiles due to its light weight (2.5 kg), small size (24×12×6 cm^3), and long-time battery supply range (8 h); this experimental design was successfully used before in other studies in an urban environment in New Zeland, and in Lower Fraser Valley in Canada (McKendry et al., 2004; Maletto et al., 2003). The OPCs may be sensitive to conditions of high relative humidity that can influence particle growth; in order to avoid any artifact in size distribution determination, only vertical profiles carried out solely in clear and dry sky conditions (RH<65%) were considered (Sjogren et al., 2008; Weingartner et

ACPD
9, 16483–16525, 2009

al., 1997). Meteorological conditions along height were measured, at the same time as particle counting and sizing, using a portable meteorological station (BABUC-ABC LSI-Lastem); pressure, temperature and relative humidity were measured with the same time resolution of particle counting. These data were used to control the relative humidity state of the atmosphere allowing us to consider only artifact-free measurements performed by the OPC.

Special sampling campaigns were carried out in the winter with a portable cascade impactor (Sioutas SKC) that allowed us to collect massive samples of particulate matter in five size stages (>2.5 μm, 1.0–2.5 μm, 0.5–1.0 μm, 0.25–0.5 μm, <0.25 μm), at different altitudes along the vertical profiles; teflon filters (Ø 25 and 37 mm, SKC) were used for PM collection and a stable flow rate of 9 l/min was guaranteed by a light weight (1 kg) battery-supplied pump (Leland Legacy pump, SKC). PM samples were analyzed by ion chromatography after 20 min of extraction in ultrapure (Milli-Q) water by ultrasonic bath (SOLTEC SONICA®) (Ferrero et al., 2008). Inorganic anions and cations were jointly analyzed by Dionex ICS-90 and an ICS-2000 coupled system equipped with: Dionex IonPac® AG14A-5 μm Guard (3×30 mm), IonPac® AS14A-5 μm Analytical column (3×150 mm), AMMS III 2 mm MicroMembrane Suppressor for anions; IonPac® CG12A-5 μm Guard (3×30 mm), IonPac® CS12A-5 μm Analytical column (3×150 mm), CMMS III 2 mm MicroMembrane Suppressor for cations. Eluent and regen for anions were Na_2CO_3/$NaHCO_3$ 8.0 mM/1.0 mM and H_2SO_4 0.05 M solutions; for cations they were MSA 20 mM and TBAOH 0.1 M. Samples were collected at ground level, into the mixing layer and over it for one hour.

At ground level, a continuous monitoring activity of PM_1 and $PM_{2.5}$ was also present using CEN equivalent (according to EN12341) samplers (FAI-Hydra dual channel low volume sampler; PTFE filters, Ø=47 mm; EU sampling inlet, 2.3 m^3/h).

2.2 Statistical data analysis and modelling

Particulate matter vertical profiles are characterised by high heterogeneity. A statistical model may be an effective tool to describe them by explicitly managing uncertainty

ACPD
9, 16483–16525, 2009

after eliciting underlying hypotheses.

In Sect. 3.3 a hierarchical Bayesian statistical model for size distribution variations along height is proposed. Parameter estimation is performed by means of simulation procedures via a Monte Carlo Markov Chain (MCMC) algorithm implemented in the OpenBugs Software for Windows (Spiegelhalter et al., 1998).

The Bayesian framework is particularly suitable for managing this kind of model (Wikle et al., 1998). The model we propose presents three levels of hierarchy: the first level constructs the data likelihood that describes the data generating process. The second level is devoted to launch-specific modelling. At the third level, the typical behaviour of a vertical profile is modelled. Each level is characterized by specific parameters. The parameter estimation is the way to obtain modelled vertical profiles, which are the main results of our proposal. The Bayesian formulation is completed by specifying prior distributions on the parameters themselves (hyperpriors on hyperparameters).

3 Results and discussion

Vertical profile measurements were carried out in Milan between 2005 and 2008 by collecting more than 300 profiles in the typical stagnant condition of the Po Valley, and providing a complete seasonal behaviour profile of aerosol properties in the lower troposphere. Measurements were mainly carried out in the morning, from sunrise to 13:00 UTC (83% of measured profiles) for characterizing at best the particle properties along height during MODIS (Moderate Resolution Imaging Spectroradiometer) Terra and Aqua overpass on the Po Valley in QUITSAT project; the remaining measurements (17%) were conducted in the afternoon until sunset. Average ground wind speed in Milan during these campaigns was very low: 0.84±0.03 m/s in the winter and 1.61±0.04 m/s in the summer. In Fig. 2a some examples from the whole vertical profile dataset are reported. Particle accumulation in the PBL (Rodriguez et al., 2007) originated a marked concentration gradient in correspondence with the mixing layer (ML)

ACPD
9, 16483–16525, 2009

height (H_{mix}) while, from the ground to the ML height, the number concentration was quite stable. Many definitions of H_{mix} are available in literature, and so mixing layer height could be determined by applying either theoretical or operational methods, the choice depends mainly on data availability. For example, potential temperature vertical profiles could be used to retrieve mixing layer height during well-mixed conditions (Holzworth, 1967; Troen et al., 1986; Holtslag et al., 1990). Assuming that atmospheric particles act like a tracer of the atmospheric dispersion state, this information contains and integrates the effects of the atmospheric physical forces (thermal and mechanical) on the particles vertical dispersion until that time during stable and convective conditions.

In this study the strongest negative particle number concentration gradient was chosen as a definition of H_{mix} (Ferrero et al., 2007a; Kim et al., 2007; Matzuki et al., 2005; McKendry et al., 2004; Maletto et al, 2003; Seibert et al., 2000). The relationship among meteorological parameters and H_{mix} will not be discussed here, as well as the comparison among different methods for accurately estimate H_{mix}. Rather, here we focus on the changes in the particle characteristics along vertical profiles, paying attention to the role of H_{mix} itself.

3.1 Number size distribution and chemical composition along height

When considering the number size distributions measured at ground level and over the ML (Fig. 3a–b) in both seasons a local minimum has been found at a particle diameter (d_p) belonging to the size class of the OPC 1.0–1.6 μm, allowing us to distinguish the vertical behaviour of the fine fraction (d_p<1.6 μm) from the coarse one (d_p>1.6 μm). On average, taking into account the total particle number concentration measured (in actual conditions of temperature and pressure) at ground level and over the ML (in the OPC size range), quite steady PM concentrations were found over the ML, representing 28±2% in the winter and 35±2% in the summer. Such behaviour describes the high capability of ML to trap primary and secondary particles into its structure, but, focusing on size distribution, we will show that the vertical dispersion of different size classes

ACPD
9, 16483–16525, 2009

is not homogeneous. The mean particle diameter of accumulation and giant nuclei modes are not constant with height. The tails of the size distributions (Fig. 3a–b) at ground level and over the ML diverge as size increases; a difference is also present for the smallest particles (the scale of Fig. 3 is logarithmic). The distribution of the ratios of the number concentrations measured above the ML, over those measured at ground level, is not constant (Fig. 4), but it is a function of particle diameter. As a first remark, the largest particles in the coarse fraction are less concentrated along height until values lower than 10%; fine particles exhibit a maximum value of this percentage in the size range 0.5–0.65 μm in the winter and 1.0–1.6 μm in the summer.

The two different behaviours for coarse and fine particles are due to different kinds of physical evolution in the atmosphere. In order to summarize the size distribution changes along height, the mean particle diameter (MPD) for the fine and the coarse fraction is calculated as:

$$\mathrm{MPD}_{=} \frac{\sum_i N_i D_i}{\sum_i N_i} \quad (1)$$

where N_i is the number concentration of particles within each size class of the OPC, and D_i its mean diameter.

In Fig. 2a–d some examples of vertical profiles of fine particles, coarse particles and their MPD along height are reported; MPD of fine and coarse fractions show opposite behaviours. Fine particles grow by passing through H_{mix}, while coarse particles MPD decrease. The two behaviours will be discussed separately.

3.1.1 Coarse fraction behaviour

Coarse particles are primarily emitted in the atmosphere by different sources (natural and anthropogenic, mainly resuspension) and they undergo dry deposition by gravitational settling (Raes et al., 2000). This basic phenomenon influences the vertical distribution behaviour in two ways.

ACPD
9, 16483–16525, 2009

First of all the vertical distribution of the coarse fraction could not be the same as the fine one. ML height (H_{mix}) was derived essentially from the fine particle vertical distribution (Fig. 2a); In fact, of the total particle number concentration (in the OPC size range) the fine fraction accounted for more than 99%, which belongs to the accumulation mode, characterized by the higher atmospheric residence time (Raes et al., 2000). The study of coarse particle vertical profiles allowed us instead to determine the mixing state (H_{coarse}) for the larger particles as well (Fig. 2c), and to compare them with the mixing layer height (Fig. 5a).

H_{mix} and H_{coarse} are highly coincident for most profiles (Fig. 5a); but, considering linear correlation in different seasons, the lowest R^2 (0.610) and the higher discrepancy of the slope (0.630) from the unit value were found in winter times; while summer times exhibited a more uniform vertical distribution of fine and coarse fractions (R^2=0.839, slope=0.934). Lower boundary layer turbulence and wind speed likely caused this phenomenon in winter times.

Atmospheric turbulence also influences coarse size distribution changes along height. Below the ML, where a certain level of turbulence was present, the MPD remained quite constant with height, but, as reported in Fig. 4, the relative contribution of the largest particles to the total coarse fraction changed with size over the ML; as a result the MPD of the coarse fraction (1) decreased (Fig. 2d) with height evidencing the sedimentation effect of the largest particles (settling velocity is a function of d^2). In particular, if the height of changing diameter for coarse particles, HCD_{coarse}, is defined as the height at which a sharp change (decrease) in the coarse MPD occurred, a strong linear relationship with H_{coarse} was found (Fig. 5b) especially in the winter (R^2=0.867, slope=1.025). In the summer this relationship was poorer (R^2=0.577, slope=0.953). On average the sedimentation process was observed in 94% of cases in the winter and in only 49% of cases in the summer. In the other cases no clear evidence in MPD decrease was found. Higher atmospheric instability weakened particle sedimentation in the summer; however less windy conditions and higher stability, in the winter, favoured particle sedimentation. The mean reduction in MPD was 14.9±0.6% and 10.7±1.0%

ACPD
9, 16483–16525, 2009

in the winter and summer respectively, with maximum reductions of 27.4% and 31.6%. Table 1 summarizes the findings above. A confirmation of sedimentation effect was obtained by correlating the percentages found over the ML, for each coarse size class, with the inverse of settling speed calculated for the same classes (R^2=0.980; Fig. 6).

These data become interesting in terms of optical effect of aerosol (i.e. Single Scattering Albedo) because different size classes characterized by different scattering and absorption efficiency are not identically vertically distributed into the mixing layer itself.

3.1.2 Fine fraction behaviour

Contrary to coarse particles, the finest ones exhibited an MPD increase at the same height of the ML (Fig. 2b). The MPD remained rather constant both within the ML and over it. The fine fraction (FF) increased its MPD in 82% of cases in the winter and only 51% in the summer. In these cases a direct comparison (Fig. 7) between H_{mix} and the height at which a sharp change (increase) in the fine MPD occurred (HCD_{fine}) showed high correlation values both in the winter (R^2=0.898, slope=1.049) and summer (R^2=0.899, slope=1.111). A mean growth in MPD of 2.1±0.1% and 3.9±0.3% in the winter and summer has been calculated, with maximum values of 6.1% and 8.5%, respectively. Table 1 also contains summary statistics for fine particle growth.

A hygroscopic growth artifact was avoided in these cases since only data with RH<65% were considered (see Table 2); in addition humidity usually decreases with height (Palchetti et al., 2008; Velasco et al., 2008; Laakso et al., 2007; Stratmann et al., 2003), and during balloon launches the ML height was characterized by a sharp decrease in the RH content. The mean RH decreasing across the ML was of 8.5±0.8%.

The FF growth over the ML was likely due to the aging process of particles in the atmosphere (i.e. coagulation and condensation). A confirmation in this direction came from the analysis of PM chemical composition along height that avoided the possibility of transport processes on days characterized by FF growth.

Samples collected at ground level, within the ML and over it on the same days in which the FF growth was evidenced, were analysed as reported in Sect. 2.1.

ACPD
9, 16483–16525, 2009

NO_3^-, SO_4^{2-} and NH_4^+ were jointly analysed and, due to the broad size ranges of the cascade impactor stages, no significant changes in their size distribution were detected along the vertical profiles; for this reason the concentrations detected in all size classes of the cascade impactor were here aggregated in order to study the vertical changes of their total atmospheric concentrations. The average atmospheric concentrations of these compounds measured respectively at ground level, into the ML and over it are summarized in Table 3. Figure 8a–c summarises the relative contribution of NO_3^-, SO_4^{2-} and NH_4^+ to their total for the aging cases; they evidenced a similar chemical composition along the whole profiles (from ground level to over the ML) supporting the theory of PM aging over the ML and discarding the presence of transport events.

On the contrary, transport events themselves were evidenced by a different MDP behaviour associated with a sharp change in chemical composition. As an example Fig. 8d–f evidences the transport event of 23 February 2007: air masses arrived over the ML from the Mediterranean sea (Fig. 8e); they were rich in sulphates (Fig. 8d), usually associated with fine particles, thus causing a sharp decrease of MDP over the ML (Fig. 8f) at the same time.

So ML height appeared in most cases as a critical parameter for splitting the lower troposphere into two areas: one, within the ML, in which fresh aerosol from anthropogenic emissions and secondary origin was present, and another one over the ML influenced by background conditions with aged aerosols (especially in the winter) or by long-range transported aerosols.

Vertical profile data were mainly collected in clear and dry sky conditions, in which aerosol properties can be derived by satellite remote sensing using different sensors (i.e. MODIS). In this case the creation of accurate look-up tables would be very useful (Levy et al., 2007; Chu et al., 2003) and could be implemented for areas with characteristics similar to the Po Valley with some parametrization to distinguish periods characterized by highly stable conditions from other periods.

The statistical model for assessing the size distribution changes of the fine fraction with height proposed in the next section establishes basis for developing a general

ACPD
9, 16483–16525, 2009

model that can predict the particle properties with height starting simply from ground (aerosol and meterological parameters) and ML measurements.

3.2 Statistical modelling of the fine fraction growth

In the previous section it has been mentioned that fine particle size distribution varies along height. The H_{mix} plays an important role, and has been estimated for each launch. The behaviour of MPD along height has been described in the previous sections. Here, focusing on the FF, we address the question of the change along height of each OPC size class relative contribution to the total count.

We propose a statistical model for the joint analysis of the proportions of PM classified according to particle size, following the theory of compositional data. Compositional data consist in parts that sum up to unity (Aitchison, 1986; Billheimer et al., 2001). In what follows, we consider the relative contribution of a specific OPC size class in the FF size range (six size classes are involved: 0.3–0.4 μm, 0.4–0.5 μm, 0.5–0.65 μm, 0.65–0.8 μm, 0.8–1.0 μm and 1.0–1.6 μm) to the total particle concentration, i.e. the sum of the number concentrations of the six size classes mentioned. Meteorological conditions are crucial antecedents for any pollutant structure: a way of taking different external conditions into account is the construction of homogenous groups by means of a clustering algorithm adapted to the treatment of compositional data (Bruno and Greco, 2008). Separate models for each group are estimated for studying the evolution of particulate matter relative size distribution along the vertical profile.

We consider 139 launches chosen among the entire dataset: a launch has been selected if its profile above the ML height can be traced. The selected launches have been clustered into 4 different typologies. Each group is characterized by very different and specific external conditions, which are summarized in Table 2. In this table the mean value per group of a series of variables is reported.

Group A and group B are formed by 39 and 56 members respectively and contain mainly winter launches whereas groups C and D contain 24 and 20 launches respectively, mainly measured on summer days. Differences between summer and winter

ACPD
9, 16483–16525, 2009

groups are evident; the mean number concentration of particles is sensibly higher in winter groups (A–B) as is the ground level pollution summarised by PM_1 and $PM_{2.5}$ levels. Since groups are made up of a high number of launches in turn characterized by a large number of observations, the estimation of models on this amount of data can be very time-consuming. If the homogeneity within a group is high, restricting the number of launches on which to estimate the model involves a sufferable loss of information, rewarded by savings in terms of computational costs. For the reasons above the prototype model for each sub-group is estimated on data from 8 launches. The eight launches selected within each group are summarised in Table 4. From this table one can check that the external conditions characterising the selected launches are similar to those of the parent groups of Table 2.

Tables 5 and 6 report the average relative size distribution within each group. Since the coarsest particles (with diameters larger than 1.6 μm) constitute less than 0.1% of the total and their atmospheric behaviour is governed by the well known sedimentation process, the first 6 (finest) size classes (0.3–1.6 μm) have been considered. The first size class constitutes more than 70% of the total counts in all groups, whereas the last three size classes account for less than 5% of the total. Groups A–B and C–D show different behaviours with respect to the second size class (0.4–0.5 μm) whose contribution is higher in winter groups (about 20%) than in summer groups (about 15%). But the more interesting observation from the table, is the predominance of the finest particles in group C. This is attributable to transport situations. Group C thus represents a cluster of vertical profiles affected by transport events; it was characterized by the lowest mean sea level pressure among the other groups (Tables 2 and 4), a condition that favours an intrusion of different air masses. These considerations apply both to the full-size groups (Table 5) and to the subsets (Table 6) selected for the successive analyses.

For each launch, the number of measurements, as well as the ML height and the maximum height reached by the balloon are different. In order to take account of the heterogeneous conditions characterising each launch, the height of each measurement

ACPD
9, 16483–16525, 2009

is considered with respect to its relative distance from the specific mixing layer height for a generic launch k ($H_{\mathrm{mix}(k)}$). Therefore, each height value has been transformed into a standardised value according to

$$X_{kh} = \frac{\mathrm{Height}_{kh} - H_{\mathrm{mix}(k)}}{H_{\mathrm{mix}(k)}} \quad (2)$$

where Height_{kh} is the height of the h-th measurement for launch k.

When exploring observed vertical profiles with respect to standardised height instead of absolute height, more homogeneous behaviours are observed. This strengthens the conjecture that H_{mix} is the crucial quantity in describing vertical profiles. In the following subsection we construct the statistical model that describes the behaviour of all size classes along height. The proposed model is able to estimate the typical vertical profile generating each launch within a group. Since data are compositional, the model has to take account of the sum-to-one constraint.

The merit of proposing a statistical approach for modelling vertical profiles consists in estimating parameters with a degree of credibility which is managed by probability. Results uncertainty can therefore be assessed and the statistical model can be used with caution, as a general paradigm.

A hierarchical model for homogeneous groups

A hierarchical model is constructed separately for each homogeneous group described in Table 6 (group-specific model). Hierarchical models are an effective tool for building complex models from relatively simple sub-models, each of them being interpreted as a level of the hierarchy. The Bayesian framework is very suitable for managing this kind of model (Wikle et al., 1998). For each group-specific hierarchical model, the variable modelled is y_{khr}, i.e. the number concentration of particles for vertical profile k, height h and size class r, (r=1,. . . ,6).

The first level of the model is:

$$\boldsymbol{y}_{kh} | \boldsymbol{p}_{kh}, n_{kh} \sim \mathrm{Multinomial}\,(\boldsymbol{p}_{kh}, n_{kh})\; k = 1, \ldots, 8;\; h = 1, \ldots, H_k \quad (3)$$

ACPD
9, 16483–16525, 2009

where $\boldsymbol{y}_{kh}$ and $n_{kh}=\sum_{r=1}^{6} y_{khr}$ are respectively a 6-dimensional vector containing the particle number concentrations and the total particle number concentrations at height h for launch k. The maximum height observed for each launch is denoted by H_k. The multinomial distribution is appropriate in this case since it permits one to model concentration data with a sum constraint (the number concentration of particles at height h for vertical profile k, denoted as n_{kh}).

Multinomial distribution is parameterised by $\boldsymbol{p}_{kh}=(p_{kh1}, p_{kh2}, \ldots, p_{kh6})$, the model parameters representing the relative contribution of each OPC size class to the whole FF number concentration. The sum to unit constraint ($\sum_{r=1}^{6} p_{khr}=1$ in Eq. 3) suggests the additive log-ratio (alr) transformation (Aitchison, 1986) for transforming parameters $\boldsymbol{p}_{kh}$ (defined in the 6-dimensional simplex space ∇^6) to the unconstrained Euclidean space $\Re^5$. We denote the transformed vector via alr function as the 5-dimensional vector $\boldsymbol{z}_{kh}=\mathrm{alr}(\boldsymbol{p}_{kh})$, where:

$$z_{khr} = \ln\left(\frac{p_{khr}}{p_{kh6}}\right) \quad r = 1, \ldots, 5 \tag{4}$$

In general, given an alr-transformed vector, back transformation from $\Re^5$ to ∇^6 is achieved via the alr^{-1} function: $\mathrm{alr}^{-1}(\boldsymbol{z}_{kh})=\boldsymbol{p}_{kh}$ where $p_{khr}=\exp(z_{khr})/\left(1+\sum_{r=1}^{5}\exp(z_{khr})\right)$ and $p_{kh6}=1/\left(1+\sum_{r=1}^{5}\exp(z_{khr})\right)$.

Further modelling regards the z_{khr} variables. Each z_{khr} is seen as a central value plus a Gaussian error with 0 mean and variance which is specific to vertical profile and size class:

$$z_{khr} = \mu_{khr} + \varepsilon_{khr} \quad \text{where} \quad \varepsilon_{khr} \sim N\left(0, \sigma_{kr}^2\right). \tag{5}$$

The mean value μ_{khr} is modelled as the sum of a constant profile-size class parameter plus a weighted sum of powers of the standardised height for describing the non

linear relationship linking X_{kh} (standardized height) and size classes:

$$\mu_{khr} = \gamma_{kr} + \sum_{j=1}^{J} \beta_{jkr} X_{kh}^{j} j = 1, \ldots, J \quad (6)$$

where γ_{kr} and $\{\beta_{jkr},\ j = 1, \ldots, J\}$ are launch specific parameters that capture the mean and shape of the r-th size class of the k-th vertical profile (with respect to the reference size class). This equation describes the behaviour of the relative contribution of the original OPC FF size classes along the standardized height. The four group-specific hierarchical models differ only in the definition of the functional relationship between vertical profile and standardised height. The degree of the polynomial is denoted by J and is chosen to be either 3 or 4 for each group-specific model.

The profile-size class parameters characterize the second level of the hierarchical model. Second level parameters are still modelled as the sum of a central value and a normal zero-mean error:

$$\beta_{jkr} = \beta_{jr} + \delta_{\beta_{jkr}} \text{ where } \delta_{\beta_{jkr}} \sim N\left(0, \sigma^2_{\beta_{jr}}\right) j = 1, \ldots, J \quad (7)$$

$$\gamma_{kr} = \gamma_{r} + \delta_{\gamma_{kr}} \text{ where } \delta_{\gamma_{kr}} \sim N\left(0, \sigma^2_{\gamma_{r}}\right) \quad (8)$$

In other words, every k-th launch-specific parameter of Eq. (6) (γ_{kr} and $\{\beta_{jkr},\ j = 1, \ldots, J\}$) is conceived as the sum of a common group parameter (γ_r and $\{\beta_{jr},\ j = 1, \ldots, J\}$) plus a random error that captures the deviation from a group-specific central value.

At the third level of hierarchy, each group is characterised by the group hyperparameters $\boldsymbol{\gamma}$ and $\boldsymbol{\beta}_j$

$$\boldsymbol{\beta}_j \left| \boldsymbol{\Sigma}_{\beta_j} \sim \text{MVN}\left(\mathbf{0}, \boldsymbol{\Sigma}_{\beta_j}\right) \right. \qquad \boldsymbol{\beta}_j : \text{ 5-dimensional vector} \quad (9)$$

$$\boldsymbol{\gamma} \,|\, \boldsymbol{\Sigma}_{\gamma} \sim \mathrm{MVN}\left(\mathbf{0}, \boldsymbol{\Sigma}_{\gamma}\right) \qquad \boldsymbol{\gamma}: \text{ 5-dimensional vector} \tag{10}$$

These group-specific parameters are the main focus of inference, because they describe the typical behaviour that characterises each group. Model hierarchy is completed by specifying Inverse Wishart distributions IW($\boldsymbol{I}$, 5) for the covariance matrices in Eqs. (9) and (10) and Inverse Gamma distributions IG (.001, 1000) for the variance parameters in Eqs. (5), (7) and (8), i.e. equivalent to non-informative priors.

Model complexity is such that analytical estimation is not feasible. Model estimation is conducted by simulation via the MCMC algorithms implemented in OpenBugs Software. Solutions are accepted after having checked convergence via the usual techniques. Inference is based on 10 000 post-convergence samples, after 30 000 burn-in iterations. The degree of the polynomial in Eq. (6) has been selected using the Deviance Information Criterion (DIC) (Spiegelhalter et al., 2002); a third grade polynomial has been chosen for groups A, B and C, while a fourth grade polynomial has been chosen for group D. In particular, transformed values $\mathrm{alr}^{-1}(\boldsymbol{\gamma})$ vectors are the model counterpart of the average relative contribution of each size class in homogeneous sub-groups entering in model estimation reported in Table 6, and their estimation is summarized in Table 7 which also reports 95% credibility intervals. Such intervals contain the empirical average relative size distribution characterising both the full-size groups (Table 5) and the subsets selected for model estimation (Table 6). This shows how statistical modelling permits one to compute measures of uncertainty of estimated values that render results more thorough than descriptive syntheses of data. Among the outputs of the hierarchical statistical model, appear the estimated MPD values corresponding to the empirical values (1). The MPD growth estimated via the model is 1.6±0.4% for group A; 2.2±0.5% for group B; −2.0±0.5% for group C and 6.1±1.2% for group D, in accordance with experimental evidence highlighted in the previous sections.

In its 4 panels, Fig. 9 reports the vertical profiles estimated via the model for each group. Profiles of the relative size distribution are represented as deviations from the

estimated γ values and centred in 1/6, which is the centre of a 6-dimensional simplex. The figure describes the shape of the prototype vertical profile for each group. This figure shows different typical behaviours of groups A, B and D, with respect to C. Results for groups A, B and D represent three models of FF growth along height. A considerable decrease in the relative contribution of the finest particles (1st size class) along height is evident. On the contrary, group C is characterized by an increase in the first size class over the ML.

However, the comparison among vertical profiles on the basis of Fig. 9 does not take account of the uncertainty characterising the results.

Uncertainty assessment can be appreciated with the help of Fig. 10, which reports 80% credibility bands for each size class in groups A (in red) and C (in blue). Credibility bands for groups B and D are not reported for sake of clarity, since they are mostly overlapped with credibility bands for group A. The ideal situation corresponding to a true discriminating model would report non-overlapping bands. This is achieved for the coarsest size class (1–1.6 μm) but not for the finest and is very evident above the ML height. Differences in graphs, rather than the interpretation of parameter values, permit one to appreciate the results of model estimation which show the unique behaviour of group C.

4 Conclusions

Climatic studies and the estimation of ground PM concentrations from satellites, require the knowledge of aerosol properties along the whole atmospheric column (Wang et al., 2003; Kaufman et al., 1983) which is a key parameter to applying inversion algorithms used to retrieve the aerosol characteristics from optical measurements. Many of those algorithms assume a vertically homogeneous atmosphere and constant aerosol optical characteristics over the whole air column (Campanelli et al., 2003; Dubovik et al., 2000).

Up to now, direct long-term particle vertical profile measurements have been scarce

ACPD
9, 16483–16525, 2009

(Penner et al., 2001) and, where they exist, they are limited to few points (Gobbi et al., 2004). In addition, due to the spatial heterogeneity of aerosol and atmospheric conditions, different behaviours of aerosol vertical properties have been described in the literature. A statistical modelling on such measurements is not available in literature.

In this paper, particulate matter vertical profile measurements, conducted at a site in the Po Valley for three years, are summarized and discussed. Vertical profiles were measured using an OPC, a meteorological station and a cascade impactor deployed on a tethered balloon. More than 300 profiles were measured between 2005 and 2008 providing a good statistical dataset.

Number size distribution and chemical composition profiles were measured along height, opening the possibility of investigating their behaviour with respect to the mixing layer height.

Fine and coarse particle size distributions showed opposite behaviour describing two different main atmospheric processes.

A settling process dominated the coarse particle profiles, in many cases causing a lower mixing state of these particles (compared to H_{mix}) and the decrease of their mean diameter.

An aging process occurred for fine particles in stable atmospheric conditions over the ML. However, transport events caused a decrease in fine fraction size.

The present study proposes a statistical model for assessing the size distribution changes of the fine fraction along height and develops a more general model able to predict particle properties along height starting from ground (aerosol and meterological) parameters and ML measurements.

Up until now we have constructed a prototype, starting from a vertical profile clustering in four homogeneous groups, where fine fraction growth along height was modelled. The hierarchical model might be improved to reduce the associated uncertainty. Further investigation is also to be performed about alternative ways to construct groups.

ML height is then a crucial parameter for splitting the lower troposphere into two areas: one, within it, in which fresh aerosol was present, and the other one, over it,

ACPD
9, 16483–16525, 2009

influenced by background conditions with aged aerosols or by long-range transported aerosols. Data on vertical profiles have a nice interpretation in terms of optical effect of aerosol (i.e. Single Scattering Albedo) because different size classes, characterized by different scattering and absorption efficiency, are not identically vertically distributed within the mixing layer itself. Usually aerosol properties can be derived by satellite remote sensing in clear and dry sky conditions, the very ones in which most vertical profiles were measured. In these cases the creation of accurate look-up tables would be very useful (Levy et al., 2007; Chu et al., 2003) and could be implemented for areas with characteristics similar to those in the Po Valley (stagnant conditions).

Acknowledgements. This paper shows some results of the Italian national QUITSAT project (Air Quality by Integrated measurements from Earth, Satellites and chemical and transport modelling; ASI financed) in which one of the main goals is to estimate PM ground concentrations from satellite data on the Po Valley domain.

This work was partially supported by the AERA foundation, Fondazione Fratelli Confalonieri, the SITECOS (MIUR financed) project and the 2006 PRIN-MIUR grant (project no. 2006139812.003, sector: Economics and Statistics).

References

Aitchison, J.: The Statistical Analysis of Compositional Data, Chapman & Hall, New York, 1986.

Amiridis, V., Melas, D., Balis, D. S., Papayannis, A., Founda, D., Katragkou, E., Giannakaki, E., Mamouri, R. E., Gerasopoulos, E., and Zerefos, C.: Aerosol Lidar observations and model calculations of the Planetary Boundary Layer evolution over Greece, during the March 2006 Total Solar Eclipse, Atmos. Chem. Phys., 7, 6181–6189, 2007, http://www.atmos-chem-phys.net/7/6181/2007/.

Billheimer, D., Guttorp, P., and Fagan, W.: Statistical Interpretation of Species Composition, J. Am. Stat. Assoc., 96, 1205–1214, 2001.

Bruno F. and Greco F.: Clustering compositional data trajectories, in: Proceedings of CODAWORK'08, The 3rd Compositional Data Analysis Workshop, edited by: Daunis-i-Estadella, J. and Martín-Fernández, J. A., 27–30 May, University of Girona, Girona (Spain), CD-ROM (ISBN: 978-84-8458-272-4), 11 pp., 2008.

Campanelli, M., Delle Monache, L., Malvestuto, V., and Olivieri, B.: On the correlation between the depth of the boundary layer and the columnar aerosol size distribution, Atmos. Environ., 37, 4483–4492, 2003.

Chu, D. A., Kaufman, Y. J., Zibordi, G., Chern, J. D., Mao, J., Chengcai, L., and Holben, B. N.: Global monitoring of air pollution over land from the Earth Observing System-Terra Moderate Resolution Imaging Spectroradiometer (MODIS), J. Geophys. Res., 108(D21), 4661, doi:10.1029/2002JD003179, 2003.

Dubovik, O., Smirnov, A., Holben, B. N., King, M. D., Kaufman, Y. J., Eck, T. F., and Slutsker, I.: Accuracy assessments of aerosol optical properties retrieved from Aerosol Robotic Network (AERONET): Sun and sky radiance measurements, J. Geophys. Res., 105, 9791–9806, 2000.

Engel-Cox, J. A., Hoff, R. M., Rogers, R., Dimmick, F., Rush, A. C., Szykman, J. J., Al-Saadi, J., Chu, D. A., and Erica, R. Z.: Integrating lidar and satellite optical depth with ambient monitoring for 3-dimensional particulate characterization, Atmos. Environ., 40, 8056–8067, 2006.

Eresmaa, N., Karppinen, A., Joffre, S. M., Räsänen, J., and Talvitie, H.: Mixing height determination by ceilometer, Atmos. Chem. Phys., 6, 1485–1493, 2006, http://www.atmos-chem-phys.net/6/1485/2006/.

Ferrero, L., Bolzacchini, E., Petraccone, S., Perrone, M. G., Sangiorgi, G., Lo Porto, C., Lazzati, Z., and Ferrini, B.: Vertical profiles of particulate matter over Milan during winter 2005/2006, Fresen. Environ. Bull., 16(6), 697–700, 2007a.

Ferrero, L., Bolzacchini, E., Perrone, M. G., Petraccone, S., Sangiorgi, G., Lo Porto, C., Ferrini, B. S., Lazzati, Z., Riccio, A., Previtali, E., Clemenza, M., Bruno, F., Cocchi, D., and Greco, F.: Influence of the Mixing Layer on the concentration and size distribution of Particulate Matter over Milan, EAC2007, Salzburg, online available at: http://www.gaef.de/EAC2007/, 2007b.

Ferrero, L., Bolzacchini, E., Perrone, M. G., Sangiorgi, G., Lo Porto, C., Ferrini, B. S., Lazzati, Z., and Petraccone, S.: Strumentazione ad ultrasuoni per la caratterizzazione chimica del particolato atmosferico, LAB, Anno XIII, October 2008 (in Italian).

Fisher, B., Kukkonen, J., Piringer, M., Rotach, M. W., and Schatzmann, M.: Meteorology applied to urban air pollution problems: concepts from COST 715, Atmos. Chem. Phys., 6, 555–564, 2006, http://www.atmos-chem-phys.net/6/555/2006/.

Gobbi, G. P., Barnaba, F., and Ammannato, L.: The vertical distribution of aerosols, Saharan

dust and cirrus clouds in Rome (Italy) in the year 2001, Atmos. Chem. Phys., 4, 351–359, 2004,
http://www.atmos-chem-phys.net/4/351/2004/.
Hayasaka, T., Meguro, Y., Sasano, Y., and Takamura, T.: Stratification and size distribution of aerosols from simultaneous measurements with a lidar, a sunphotometer, and an aureolameter, Appl. Optics, 37, 961–970, 1998.
Hinds, W. C.: Aerosol Technology, Wiley-Interscience edition, 1999.
Holtslag, A. A. M., De Bruin, E. I. F., and Pan, H.-L.: A high resolution air mass transformation model for short range weather forecasting, Mon. Weather Rev., 118, 1561–1575, 1990.
Holzworth, C. G.: Mixing depths, wind speeds and air pollution potential for selected locations in the United States, J. Appl. Meteorol., 6, 1039–1044, 1967.
IPCC: Climate Change 2007, onliine available at: http://www.ipcc.ch/publications_and_data/publications_and_data_reports.htm, 2007.
Kaufman, Y. J., and Fraser, R. S.: Light Extinction by Aerosols During Summer Air Pollution, J. Appl. Meteorol., 22, 1694–1706, 1983.
Kaufman, Y. J., Tanré, D., and Boucher, O.: A satellite view of aerosols in the climate system, Nature, 419, 215-223, 2002.
Kim, S. W., Yoon, S. C., Won, J. G., and Choi, S. C.: Ground-based remote sensing measurements of aerosol and ozone in an urban area: A case study of mixing height evolution and its effect on ground-level ozone concentrations, Atmos. Environ., 41, 7069–7081, 2007.
Koren, I., Kaufman, Y. J., Remer, L. A., and Martins, J. V.: Measurments of the effect of amazon smoke on inhibition of cloud formation, Scienze, 303, 1342–1345, 2004.
Laakso, L., Grönholm, T., Kulmala, L., Haapanala, S., Hirsikko, A., Lovejoy, E. R., Kazil, J., Kurtén, T., Boy, M., Nilsson, E. D., Sogachev, A., Riipinen, I., Stratmann, F., and Kulmala, M.: Hot air balloon as a platform for boundary layer profile measurements during particle formation, Boreal Environ. Res., 12, 279–294, 2007.
Levy, R. C., Remer, L. A., Mattoo, S., Vermote, E.,F., and Kaufman, Y. J.: Second generation operational algorithm: Retrieval of aerosol properties over land from inversion of Moderate Resolution Imaging Spectroradiometer spectral reflectance, J. Geophys. Res., 112, D13211, doi:10.1029/2006JD007811, 2007.
Liu, Y., Sarnat, J. A., Kilaru, V., Jacob, D. J., and Koutrakis, P.: Estimating ground-level $PM_{2.5}$ in the Eastern United States using satellite remote sensing, Environ. Sci. Technol., 39, 3269–3278, 2005.

Liu, Y., Franklin, M., Kahn, R., and Koutrakis, P.: Using aerosol optical thickness to predict ground-level $PM_{2.5}$ concentrations in the St. Louis area: A comparison between MISR and MODIS, Remote Sens. Environ., 107, 33–44, 2007.

Maletto, A., McKendry, I. G., and Strawbridge, K. B.: Profiles of particulate matter size distributions using a balloon-borne lightweight aerosol spectrometer in the planetary boundary layer, Atmos. Environ., 37, 661–670, 2003.

Matzuki, A., Iwasaka, Y., Shi, G.-Y., Chen, H.-B., Osada, K., Zhang, D., Kido, M., Inomata, Y., Kim, Y.-S., Trochkine, D., Nishita, C., Yamada, M., Nagatani, T., and Nakata, H.: Heterogeneous Sulphate formation on dust surface and its dependence on mineralogy: balloon-borne observations from balloon-borne measurements in the surface atmosphere of Beijing, China, Water Air Soil Poll., 5, 101–132, 2005.

McKendry, I. G., Sturman, A. P., and Vergeiner, J.: Vertical profiles of particulate matter size distributions during winter domestic burning in Christchurch, New Zealand, Atmos. Environ., 38, 4805–4813, 2004.

Penner, J. E., Andreae, M., Annegarn, H., Barrie, L., Feichter, J., Hegg, D., Jayaraman, A., Leaitch, R., Murphy, D., Nganga, J., and Pitari, G.: Aerosols, their Direct and Indirect Effects, In Climate Change 2001: The Scientific Basis, Cambridge University Press, Cambridge, UK, 2001.

Palchetti, L., Bianchini, G., Carli, B., Cortesi, U., and Del Bianco, S.: Measurement of the water vapour vertical profile and of the Earth's outgoing far infrared flux, Atmos. Chem. Phys., 8, 2885–2894, 2008, http://www.atmos-chem-phys.net/8/2885/2008/.

Pope, C. and Dockery, D.: Chapter 31. Epidemiology of particle effects, in: Air pollution and health, edited by: Holgate, S. T., Koren, H. S., Samet, J. M., and Maynard, R. L., Academic Press, San Diego, 673–705, 1999.

Raes, F., Van Dingenen, R., Vignati, E., et al.: Formation and cycling of aerosols in the global troposphere, Atmos. Environ., 34, 4215–4240, 2000.

Rodríguez, S., Van Dingenen, R., Putaud, J.-P., Dell'Acqua, A., Pey, J., Querol, X., Alastuey, A., Chenery, S., Ho, K.-F., Harrison, R., Tardivo, R., Scarnato, B., and Gemelli, V.: A study on the relationship between mass concentrations, chemistry and number size distribution of urban fine aerosols in Milan, Barcelona and London, Atmos. Chem. Phys., 7, 2217–2232, 2007, http://www.atmos-chem-phys.net/7/2217/2007/.

Rojas-Bracho, L., Suh, H., and Koutrakis, P.: Relationships among personal, indoor, and outdoor fine and coarse particle concentrations for individuals with COPD, J. Expo. Anal. Env. Epid., 10(3), 294–306, 2000.
Sarigiannis, D. A., Soulakellis, N. A., and Sifakis, N. I.: Information fusion for computational assessment of air quality and health effects, Photogramm. Eng. Rem. S., 70(2), 235–245, 2004.
Schwartz, J., Dockery, D., and Neas, L.: Is daily mortality associated specifically with fine particles?, J. Air Waste Manage., 46(10), 927–939, 1996.
Seibert, P, Beyrich, F., Gryning, S. E., Joffre, S., Rasmussen, A., and Tercier, P.: Review and intercomparison of operational methods for the determination of the mixing height, Atmos. Environ., 34, 1001–1027, 2000.
Seinfeld, J. H. and Pandis, S. N.: Atmospheric chemistry and physics – From air pollution to climate change, Wiley-Interscience edition, 1998.
Schaap, M., Apituley, A., Timmermans, R. M. A., Koelemeijer, R. B. A., and de Leeuw, G.: Exploring the relation between aerosol optical depth and $PM_{2.5}$ at Cabauw, the Netherlands, Atmos. Chem. Phys., 9, 909–925, 2009, http://www.atmos-chem-phys.net/9/909/2009/.
Sjogren, S., Gysel, M., Weingartner, E., Alfarra, M. R., Duplissy, J., Cozic, J., Crosier, J., Coe, H., and Baltensperger, U.: Hygroscopicity of the submicrometer aerosol at the high-alpine site Jungfraujoch, 3580 m a.s.l., Switzerland, Atmos. Chem. Phys., 8, 5715–5729, 2008, http://www.atmos-chem-phys.net/8/5715/2008/.
Spiegelhalter, D. J., Best, N., Carlin, B. P., and Van der Linde, A.: Bayesian measures of model complexity and fit (with discussion), J. R. Stat. Soc. B, 64, 583–639, 2002.
Spiegelhalter, D., Thomas, A., and Best, N.: WinBugs: Bayesian inference using Gibbs sampler, Manual Version 1.2. Imperial College, London and Medical Research Council Biostatistics Unit, Cambridge, 1998.
Stratmann, F., Siebert, H., Spindler, G., Wehner, B., Althausen, D., Heintzenberg, J., Hellmuth, O., Rinke, R., Schmieder, U., Seidel, C., Tuch, T., Uhrner, U., Wiedensohler, A., Wandinger, U., Wendisch, M., Schell, D., and Stohl, A.: New-particle formation events in a continental boundary layer: first results from the SATURN experiment, Atmos. Chem. Phys., 3, 1445–1459, 2003, http://www.atmos-chem-phys.net/3/1445/2003/.
Taubman, B. F., Hains, J. C., Thompson, A. M., Marufu, L. T., Doddrige, B. G., Stehr, J. W., Piety,

C. A., and Dickerson, R. R.: Aircraft vertical profiles of trace gas and aerosol pollution over the mid-Atlantic United States: statistics and meteorological cluster analysis, J. Geophys. Res., 111, D10S07, doi:10.1029/2005JD006196, 2006.

Troen, I. and Mahrt, L.: A simple model of the atmospheric boundary layer model; sensitivity to surface evaporation, Bound.-Lay. Meteorol., 37, 129–148, 1986.

Van Dingenen, R., Raes, F., Putaud, J. P., et al.: A European aerosol phenomenology-1: physical characteristics of particulate matter at kerbside, urban, rural and background sites in Europe, Atmos. Environ., 38, 2561–2577, 2004.

Velasco, E., Márquez, C., Bueno, E., Bernabé, R. M., Sánchez, A., Fentanes, O., Wöhrnschimmel, H., Cárdenas, B., Kamilla, A., Wakamatsu, S., and Molina, L. T.: Vertical distribution of ozone and VOCs in the low boundary layer of Mexico City, Atmos. Chem. Phys., 8, 3061–3079, 2008, http://www.atmos-chem-phys.net/8/3061/2008/.

Vecchi, R., Marcazzan, G., Valli, G., Cerini, M., and Antoniazzi, C.: The role of atmospheric dispersion in the seasonal variation of PM1 and $PM_{2.5}$ concentration and composition in the urban area of Milan (Italy), Atmos. Environ., 38, 4437–4446, 2004.

Wang, J. and Christofer, S. A.: Intercomparison between satellite-derived aerosol optical thickness and $PM_{2.5}$ mass: Implications for air quality studies, Geophys. Res. Lett., 30(21), 2095, doi:10.1029/2003GL018174, 2003.

Weingartner, E., Burtscher, H., and Baltensperger, U.: Hygroscopic properties of carbon and diesel soot particles, Atmos. Environ., 31(15), 2311–2327, 1997.

Wikle, C. K., Berliner, L. M., and Cressie, N.: Hierarchical Bayesian space-time models, Environ. Ecol. Stat., 5 , 117–154, 1998.

Table 1. Statistics for MPD changes during aging and sedimentation processes. FFG=Fine Fraction Growth, CFR=Coarse Fraction Reduction.

MPD relative changes	Winter		Summer	
	FFG %	CFR %	FFG %	CFR %
mean	2.1	14.9	3.9	10.7
σ_m	0.1	0.6	0.3	1.0
σ	1.3	6.1	1.7	7.5
min	0.3	1.8	0.3	1.4
25° perc	1.0	11.0	2.8	4.5
50° perc	1.8	14.3	3.3	9.1
75° perc	2.9	19.6	5.2	15.3
max	6.1	27.4	8.5	31.6

Table 2. Descriptive statistics for each homogeneous group.

	Nr. of Launches	Mean Part. conc. (cm^{-3})	MLH (m)	Temp. (°C)	Humid. (%)	Pressure (hPa)	PM_1 ($\mu g/m^3$)	$PM_{2.5}$ ($\mu g/m^3$)
Group A	39	425.7	144.62	4.79	63.78	1006.27	38.78	104.41
Group B	56	428.5	240.75	7.99	56.09	972.31	28.79	80.66
Group C	24	81.84	279.92	19.00	51.57	940.21	20.55	38.39
Group D	20	58.31	203.80	23.07	44.73	977.51	14.89	28.59

ACPD
9, 16483–16525, 2009

Table 3. Mean atmospheric concentrations for NO_3^-, SO_4^{2-} and NH_4^+ measured along vertical profiles.

Atmospheric concentrations ($\mu g/m^3$)	NO_3^- mean	σm	SO_4^{2-} mean	σm	NH_4^+ mean	σm
Ground	22.3	2.9	6.8	1.7	7.0	0.5
Into the ML	23.0	4.9	6.8	1.6	5.9	0.6
Over the ML	8.8	2.9	3.0	1.1	3.0	0.7

ACPD
9, 16483–16525, 2009

Table 4. Descriptive statistics for homogeneous sub-groups entering in model estimation.

	Nr. of Launches	Mean Part. conc. (cm^{-3})	MLH (m)	Temp. (°C)	Humid. (%)	Pressure (hPa)	PM_1 ($\mu g/m^3$)	$PM_{2.5}$ ($\mu g/m^3$)
Group A	8	393.6	132.13	5.37	62.59	1001.59	34.67	105.13
Group B	8	445.5	261.75	3.24	56.90	974.51	39.00	78.88
Group C	8	46.04	281.25	10.95	51.52	982.80	18.40	29.82
Group D	8	64.45	243.25	23.30	42.17	974.24	14.29	26.81

ACPD
9, 16483–16525, 2009

Table 5. Average size distribution in the homogeneous groups.

	Nr. of Launches	0.3–0.4 μm	0.4–0.5 μm	0.5–0.65 μm	0.65–0.8 μm	0.8–1 μm	1–1.6 μm
Group A	39	0.7340	0.2101	0.0443	0.0075	0.0031	0.0010
Group B	56	0.7158	0.2201	0.0503	0.0087	0.0038	0.0012
Group C	24	0.7822	0.1507	0.0381	0.0131	0.0106	0.0053
Group D	20	0.7336	0.1569	0.0576	0.0234	0.0195	0.0090

ACPD
9, 16483–16525, 2009

Table 6. Average size distribution in homogeneous sub-groups entering in model estimation.

	Nr. of Launches	0.3–0.4 μm	0.4–0.5 μm	0.5–0.65 μm	0.65–0.8 μm	0.8–1 μm	1–1.6 μm
Group A	8	0.7139	0.2285	0.0470	0.0069	0.0028	0.0009
Group B	8	0.7259	0.2152	0.0458	0.0081	0.0037	0.0013
Group C	8	0.8029	0.1384	0.0346	0.0117	0.0084	0.0040
Group D	8	0.7357	0.1573	0.0559	0.0227	0.0194	0.0089

ACPD
9, 16483–16525, 2009

Table 7. Posterior credibility intervals of $\text{alr}^{-1}(\boldsymbol{\gamma})$, i.e. the estimated average size distribution.

	0.3–0.4 μm	0.4–0.5 μm	0.5–0.65 μm	0.65–0.8 μm	0.8–1 μm	1–1.6 μm
Group A	0.7151	0.2272	0.0466	0.0072	0.0028	0.0009
	(0.6941,0.7669)	(0.1682,0.2763)	(0.0329,0.0597)	(0.0054,0.0093)	(0.0023,0.0034)	(0.0008,0.001)
Group B	0.7214	0.2171	0.0479	0.0078	0.0031	0.0011
	(0.6581,0.778)	(0.1757,0.2867)	(0.0351,0.0651)	(0.006,0.0103)	(0.0025,0.0038)	(0.0009,0.0015)
Group C	0.7989	0.1401	0.0341	0.0109	0.0081	0.0037
	(0.7616,0.8303)	(0.1165,0.1768)	(0.0279,0.0416)	(0.0092,0.0129)	(0.0069,0.0097)	(0.0033,0.0042)
Group D	0.7336	0.1586	0.0517	0.0207	0.0181	0.0074
	(0.6205,0.7976)	(0.1005,0.2348)	(0.0313,0.0827)	(0.0127,0.0284)	(0.0104,0.0201)	(0.0061,0.0091)

ACPD
9, 16483–16525, 2009

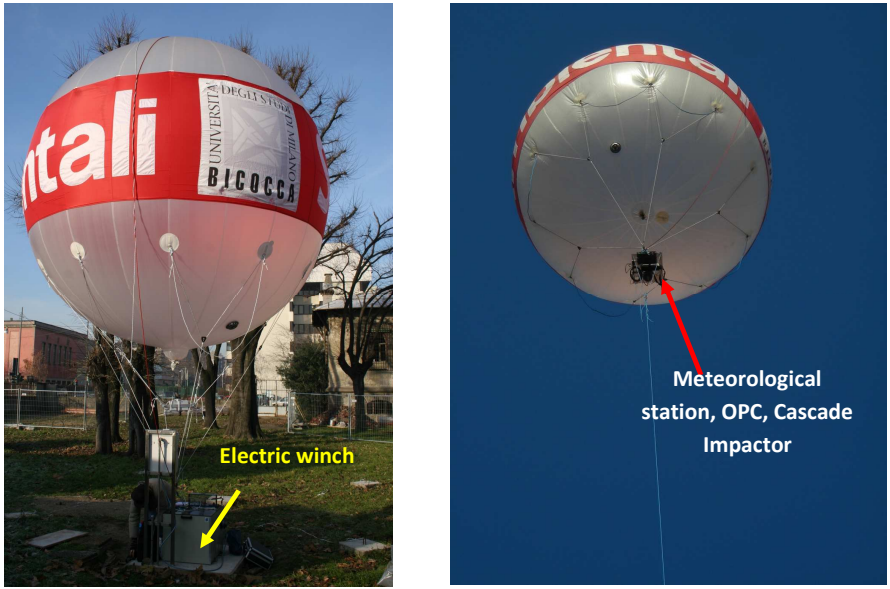

Fig. 1. The tethered balloon before launching at the sampling site and during a flight with its payload.

ACPD
9, 16483–16525, 2009

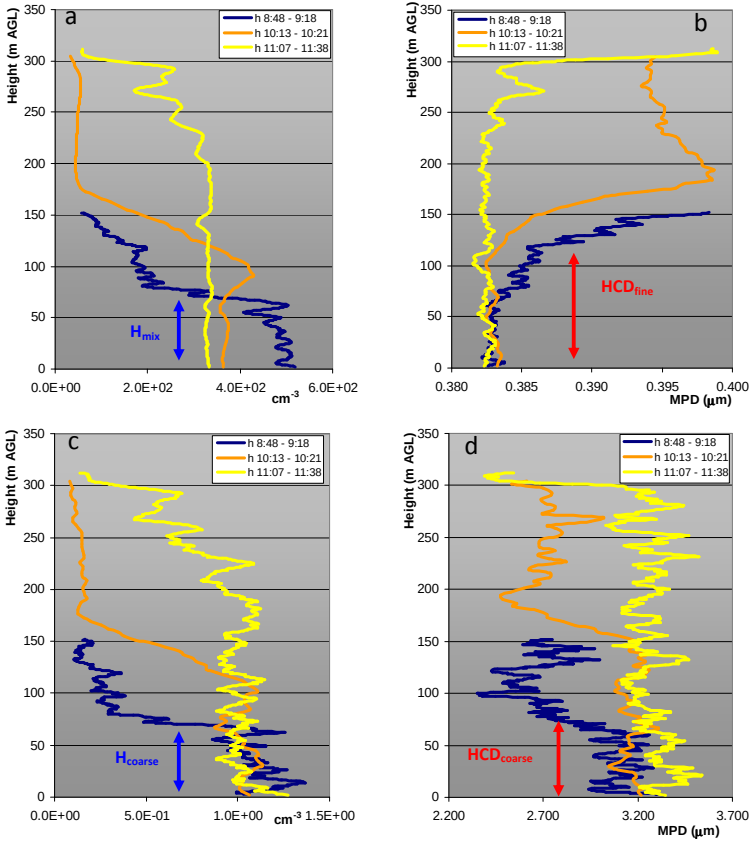

Fig. 2. Vertical profiles of the particle number concentration and the Mean Particle Diameter (MPD) on 20 December 2005; number concentration and the MPD for the fine particles are reported in **(a)** and **(b)**, respectively, while the number concentration and the MPD for the coarse fraction are reported in **(c)** and **(d)**, respectively.

ACPD
9, 16483–16525, 2009

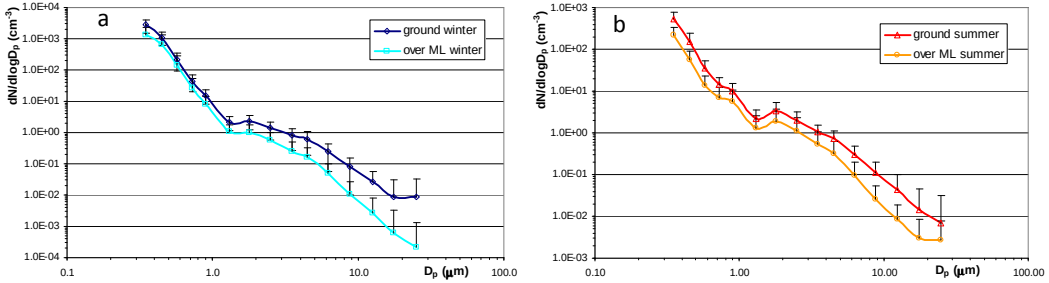

Fig. 3. Number size distributions of particulate matter at ground level both in winter **(a)** and summer **(b)** campaigns.

ACPD
9, 16483–16525, 2009

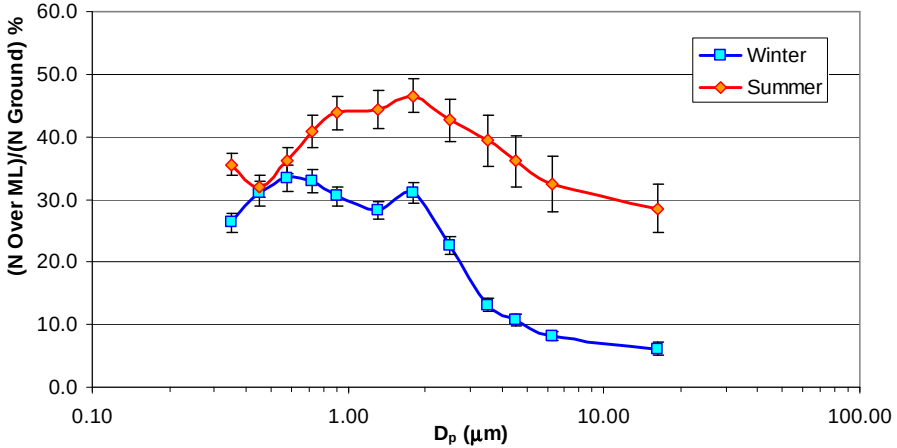

Fig. 4. Percentage of the particle number concentration measured over the mixing layer referred to those at ground level in function of size.

ACPD
9, 16483–16525, 2009

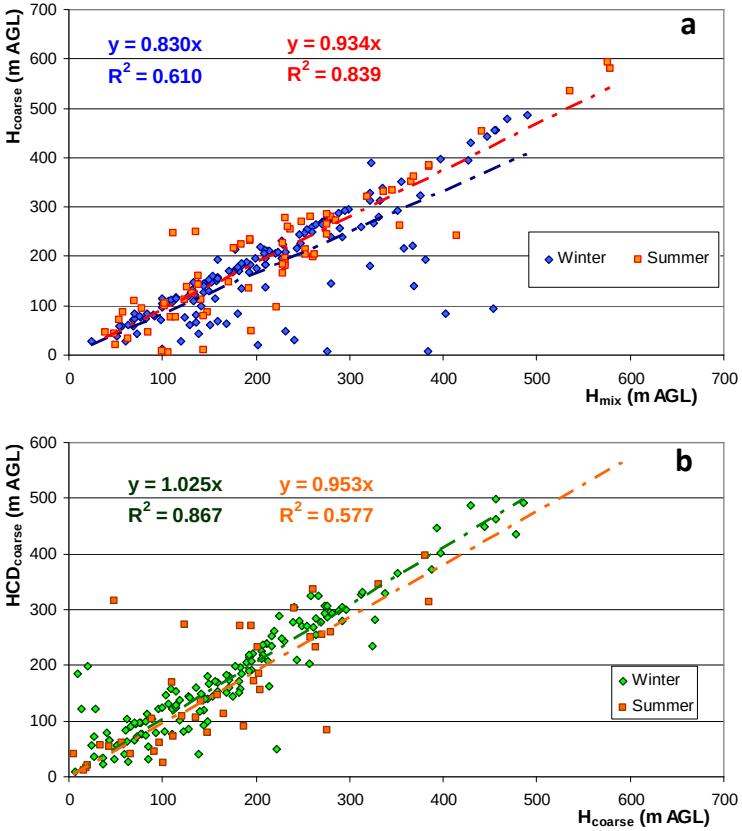

Fig. 5. Linear correlation among H_{mix} and H_{coarse} **(a)**, and among H_{coarse} and HCD_{coarse} in the winter and summer.

ACPD
9, 16483–16525, 2009

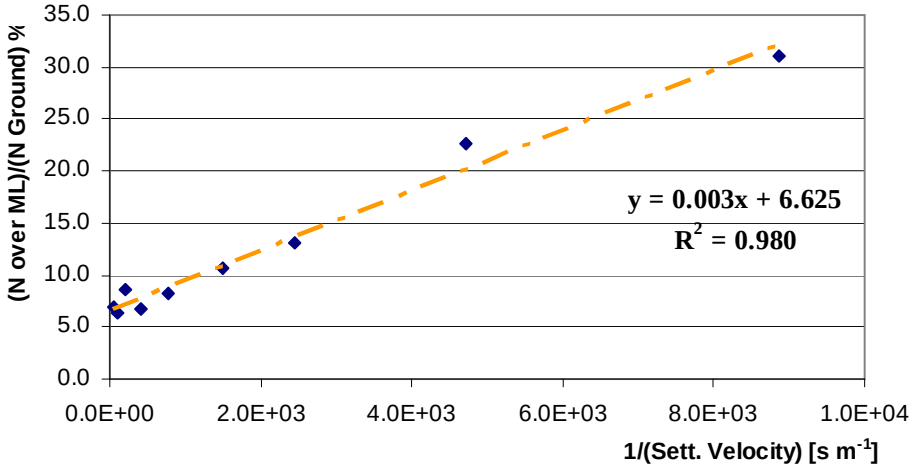

Fig. 6. Linear correlation between the percentage over the ML of each coarse size class and the reciprocal of settling velocity.

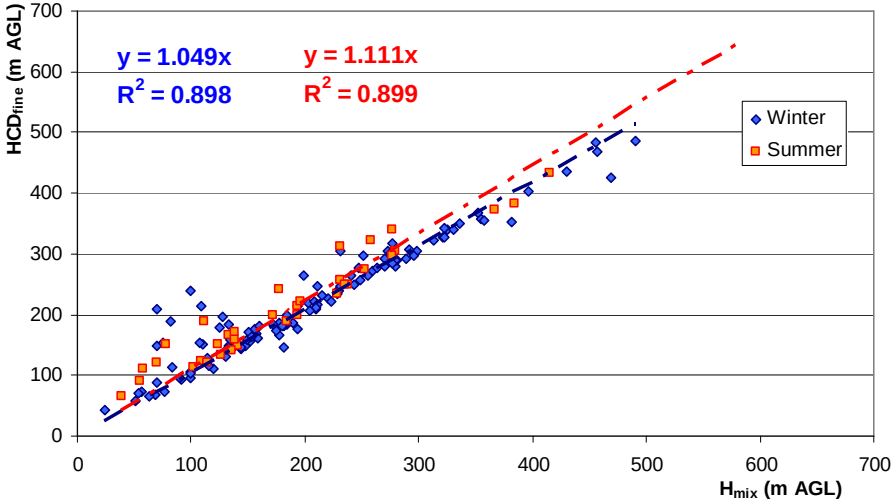

Fig. 7. Linear correlation between H_{mix} and HCD_{fine} for winter and summer.

ACPD
9, 16483–16525, 2009

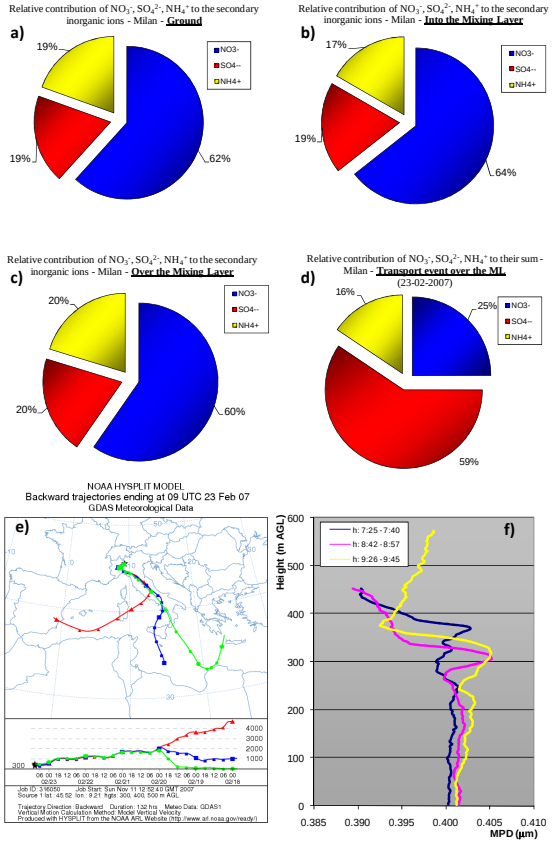

Fig. 8. (a–c) Average NO_3^-, SO_4^{2-} and NH_4^+ relative values at ground level, within the ML and over it during FF growth. **(d)** NO_3^-, SO_4^{2-} and NH_4^+ relative values during a transport event. **(e–f)** back trajectories and MPD during the transport event.

ACPD
9, 16483–16525, 2009

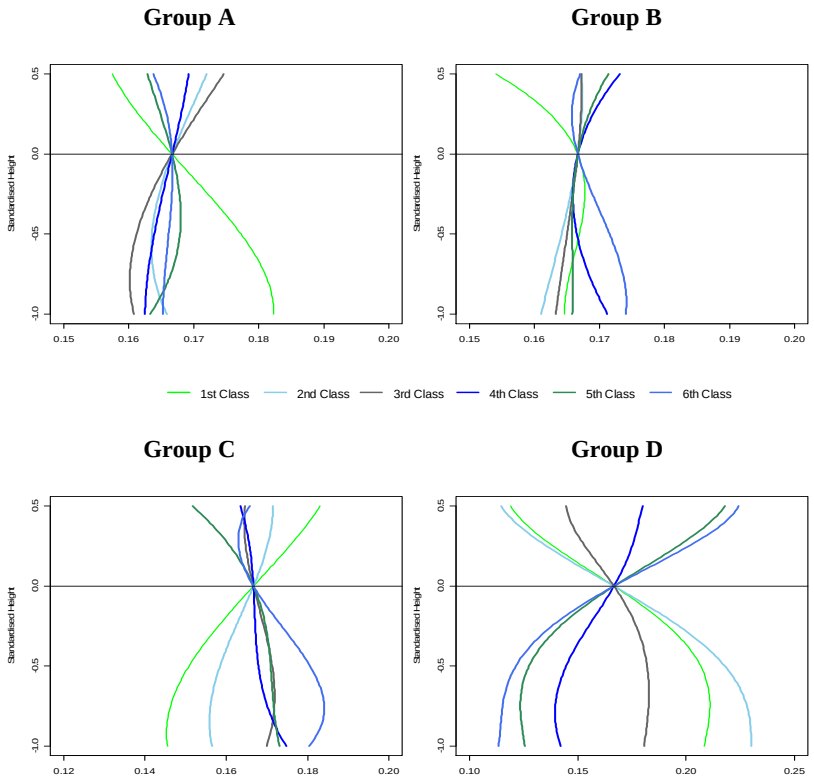

Fig. 9. Typical centred vertical profiles estimated via the statistical hierarchical model.

ACPD
9, 16483–16525, 2009

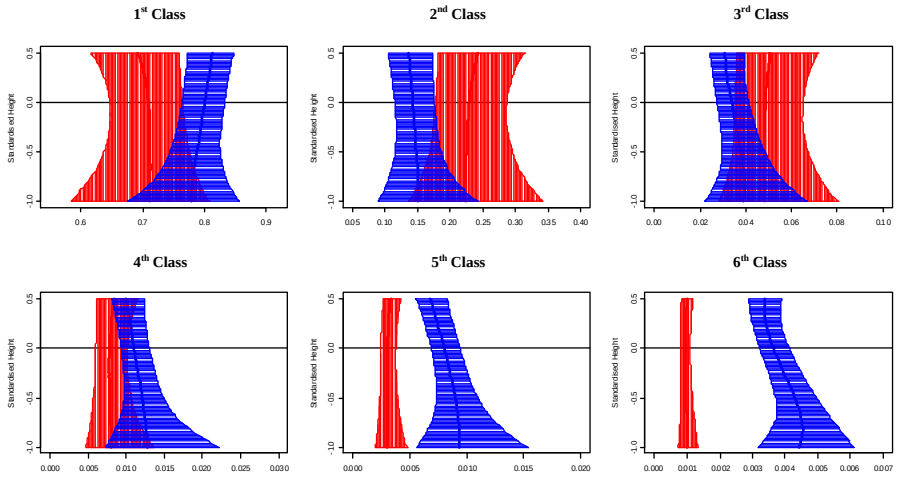

Fig. 10. 80% credibility bands for typical vertical profiles estimated for groups A (red) and C (blue).

ACPD
9, 16483–16525, 2009